Unravelling Kinetic and Thermodynamic Effects on the Growth of Gold Nanoplates by Liquid Transmission Electron Microscopy

Damien Alloyeau,[1]* Walid Dachraoui,[1] Yasir Javed,[1] Hannen Belkahla,[2] Guillaume Wang,[1] Hélène Lecoq[2], Souad Ammar,[2] Ovidiu Ersen,[4] Andreas Wisnet,[5] Florence Gazeau,[3] Christian Ricolleau.[1]

[1] Laboratoire Matériaux et Phénomènes Quantiques, UMR 7162 CNRS/Université Paris - Diderot, 10 rue Alice Domon et Léonie Duquet, 75013 Paris, France.

[2] Interfaces Traitements Organisation et Dynamique des Systèmes, UMR7086 CNRS/Université Paris - Diderot, 15, rue Jean-Antoine de Baïf, 75013 Paris, France.

[3] Laboratoire Matières et Systèmes Complexes, UMR 7057 CNRS/Université Paris - Diderot, 10 rue Alice Domon et Léonie Duquet, 75013 Paris, France.

[4] Institut de Physique et Chimie des Matériaux de Strasbourg (IPCMS, UMR 7504 CNRS-UDS), 23 rue du Loess BP 43 F-67034, Strasbourg Cedex 2, France.

[5] Department of Chemistry and CeNS, Ludwig-Maximilians-University, Butenandtstr. 11, 81377 Munich, Germany.

* Corresponding author email: damien.alloyeau@univ-paris-didrot.fr

Experimental details:

Liquid sample preparation

The liquid cells commercialized by Protochips Inc. consist of two silicon wafers with dimensions of 2 * 2 mm and 4.5 * 6 mm, called the small and large E-chips respectively (Fig. S1). Each E-chip has one 550 µm * 50 µm window covered by a 30 nm thick Si_3N_4 amorphous film. A 2.5 µL drop of $HAuCl_4$ aqueous solution (1 mM), prepared using a commercial solution (Sigma-Aldrich, Au 49% min), was deposited on the electron transparent Si_3N_4 membrane of the small E-chip. Note that plasma cleaning procedure prior to loading improve the wettability of the devices. The large E-chip was then placed over the small one with their windows in cross-configuration, giving a square field of view of 50 µm edge length. Therefore, the drop of solution was squeezed in between the two E-Chips in a volume defined by the thickness of the gold spacers on the small E-Chip (150 nm in our case). The entire chamber was then closed by the lid of the holder tip resulting in a vacuum sealed liquid-cell. As illustrated in Figure S1, the impermeability of the liquid cell is ensured by two concentric O-rings. We did not use the holder in flow mode. Note that in the JEOL ARM microscope the liquid cell is upside down (small E-chip on the top).
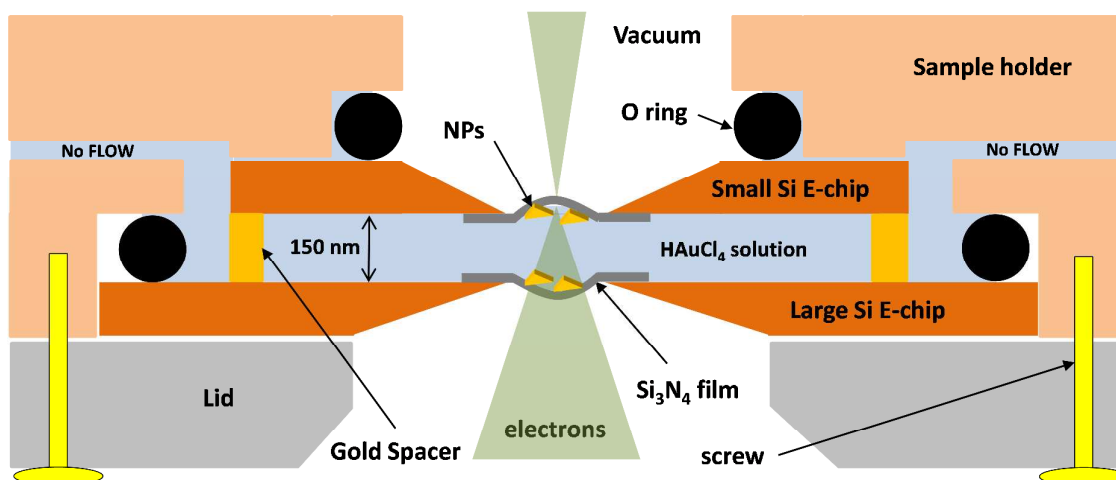
Figure S1: Schematic cross section of the sealed liquid cell in the JEOL ARM microscope (small E-chip on the top).

All the TEM experiments were realized on the JEOL ARM 200F microscope equipped together with a CEOS aberration corrector for the objective lens and cold FEG. All the experiments were performed with a 200 kV acceleration voltage.

***In situ* STEM imaging**

STEM HAADF imaging was performed by using the smallest probe size (8c) and the smallest condenser aperture (10 µm) in order to minimize and maintain a constant beam current (i_e). The latter was measured on the phosphorescent screen of the microscope prior to insert the sample to determine the dose rate focalized on the liquid cell ($i_e = 1.24 \ 10^8$ electron/s or 19.8 pA). NPs growth was followed by continuously recording 1024*1024 images with a pixel dwell time of 25 µs.

The thickness of the spacers corresponds to the smallest liquid thickness crossed by the electron beam during the TEM experiment. Indeed due to the outward bowing of the Si_3N_4 membranes under vacuum (Figure S1), the smallest liquid thickness is found at the corners of the viewing window, where all the image series were recorded. As illustrated in the main text,

the NPs were formed on the Si_3N_4 membrane and they stayed under electron beam irradiation. This affinity of the growing gold NPs for the membrane was an essential condition for visualizing the growth of individual nanostructures over several minutes. In order to improve resolution and signal to noise of STEM imaging, the probe was focused on the upper Si_3N_4 membrane (small E-Chip) during the growth experiment, but we observed the formation of gold NPs on both E-chip windows.

Ex situ analyses

SEM, HRTEM, STEM-HAADF and tomography experiments were realized on the small E-chips after unsealing the liquid-cell. High-resolution SEM imaging was realized on a Zeiss SUPRA 40 microscope equipped with a field-emission gun and an Everhart Thornley Detector. We performed imaging with tilting angle up to 65° to qualitatively observe the large thickness difference between planar and 3D nanoparticles.

As the dimensions of the small E-chip are close to the diameter of a conventional TEM grid, aberration-corrected HRTEM and STEM HAADF analysis were realized with a conventional TEM Holder. For quantitative analyses of STEM HAADF contrast, all the images were intentionally acquired with very small camera length in order to collect the very high angle scattering electrons. These optical conditions minimize diffraction contrast which varies with the orientation of the nanoparticles. Note that the slight contribution of these diffraction effects will be the same for all the nanoplates since they were all oriented along the [111] zone axis orientation. In all images, we used the signal to noise ratio (SNR) definition proposed by Rose. *[Rose et al. Advances in Electronics and Electron Physics (1948) 131–166]* The SNR corresponds to the incremental change in the image intensity due to NPs and the noise is the standard deviation (σ) of the membrane intensity (I_0).

$$SNR = \frac{I - I_0}{\sigma}$$

For tomography acquisition, the small E-chip was glued on the tip of the Gatan tomography holder (Fig. S2a). In spite of this unusual sample, the tilt range in the UHR pole piece of the ARM microscope remains large enough for 3D reconstruction. A tomography data set consisting of 134 STEM HAADF images was collected between -60° and +54° using the Saxton scheme, where the tilt increment depends on the cosine of the overall tilt angle. After a fine alignment of all projections, the 3D volume was calculated using the discrete algebraic reconstruction technique (DART). For this purpose, a preliminary simultaneous iterative reconstruction technique (SIRT) reconstruction was performed [Zürner et al. Ultramicroscopy 2012, 115, 41-49]. By constraining the reconstruction volume with a mask which roughly equals the particles shapes, reliable material densities can be deduced. Subsequently, the density for the gold particles is used to perform a DART reconstruction, which is discrete in terms of gray values. [Batenburg et al. Ultramicroscopy 109, 730 (2009)] This means that each voxel (unit fragment of the volume) is attributed to either vacuum or gold. Consequently, DART is superior to SIRT when exact particle boundaries are to be determined. Volume rendering and thickness measurements in the tomogram were performed by using Imod software.

Additional data:

Table S1

Nanostructure type	Probability	Possible shape transition	Comments
2-4 nm truncated octahedrons	NA	3D multi-twins NPs or planar NPs	These small Wulff polyhedrons systematically evolve towards larger multi-twins structures with 3D or planar geometries
Triangular nanoplates	1.4 %	Hexagonal nanoplates	Many originally triangular nanoplates evolve towards truncated triangles or hexagonal nanoplates
Truncated-triangle nanoplates	3.5%	Hexagonal nanoplates	We observed the formation of truncated triangles due to a late transition from triangular towards hexagonal nanoplates. The size of the three pre-existing facets is not overcome by the three other facets growing after the transition
Hexagonal nanoplates	9.1%	No shape transition	When nanoplates reach hexagonal shape they keep growing with the same six-fold symmetry
3D multi-twins icosahedral or decahedral NPs	86%	No shape transition	When the growth tends towards 3D nanostructures we did not observe any transition back to planar geometry

Summary of *ex situ* and *in situ* observations. Probability of observation are deduced from statistical analyses over 1000 particles observed *ex situ*.
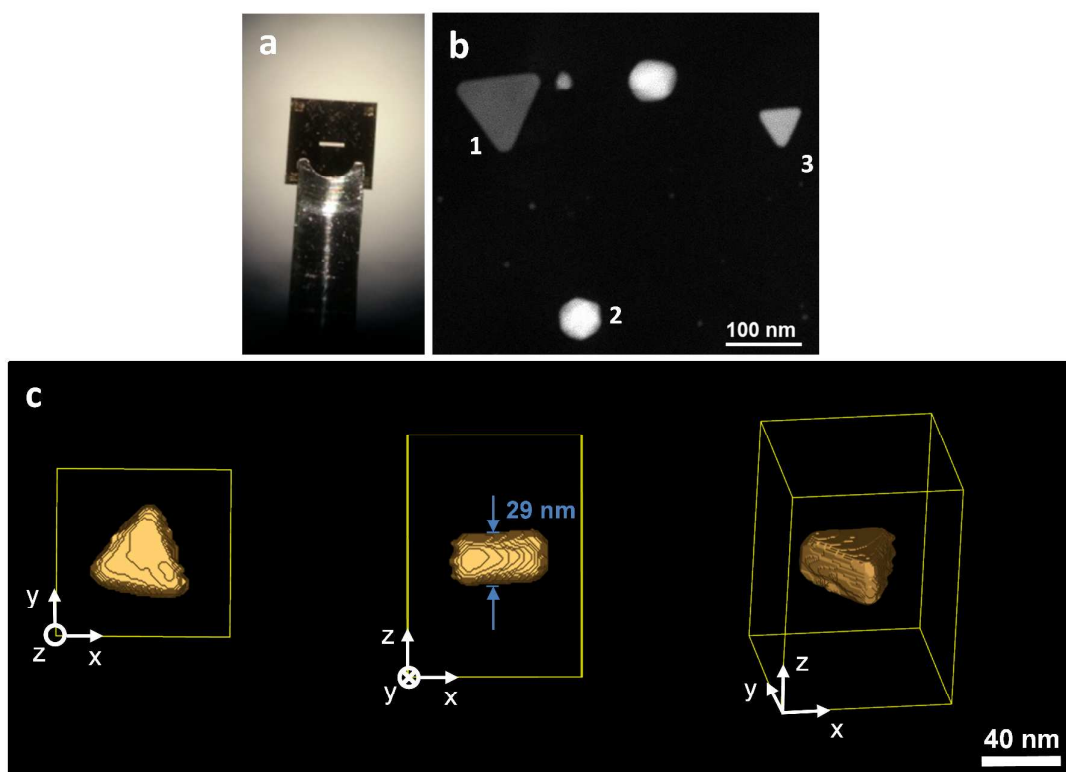
Figure S2: *Ex situ* electron tomography. (a) Picture of the small E-chip glued on the tip of the Gatan tomography holder. (b) STEM HAADF image extracted from the tilt series of tomography experiment (close to 0° tilt). NPs labelled 1, 2 and 3 correspond to the tomograms seen in figures 2b, 2c and S2c, respectively. (c) 3D DART reconstruction calculated from electron tomography experiments. From left to right: top view, side view and 3D view of a nanoprism with an edge length of 52 nm and a thickness of 29 nm.
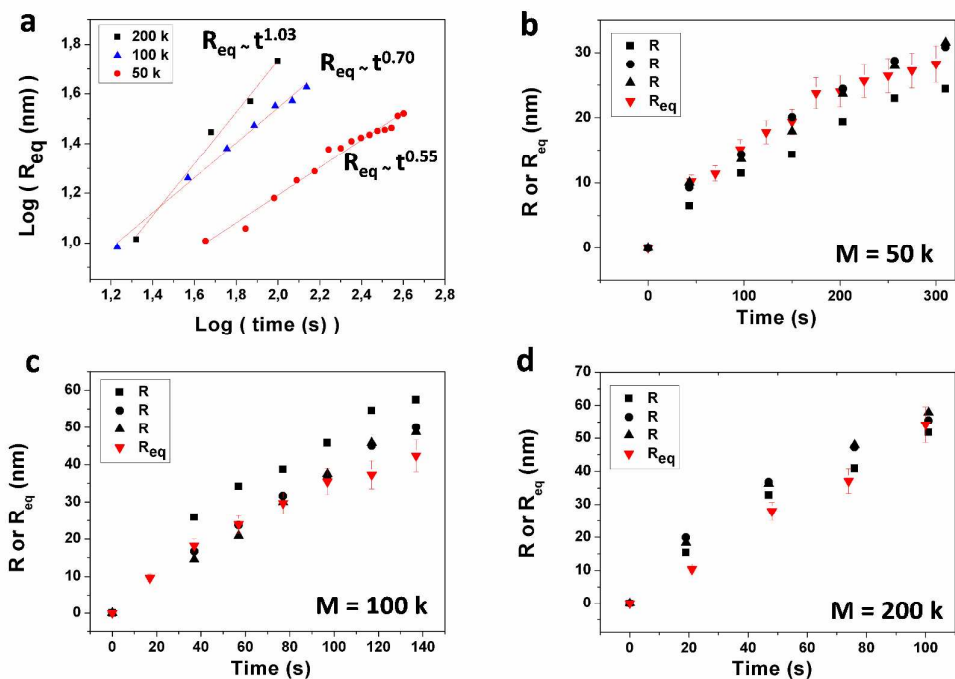
Figure S3: Comparing the growth of planar and 3D NPs. (a) Logarithmic relationships between the equivalent radius of average-sized nanoplates (R_{eq}) and time for magnifications 50k, 100k and 200k. Equivalent radius of average-size nanoplates (R_{eq}, red triangles) and radius of three average-sized 3D NPs (R, black data points) as a function of time for magnifications (b) 50 k, (c) 100 k and (d) 200 k. Error bars on R_{eq} data are due to the thickness dispersion measured on the nanoplates.
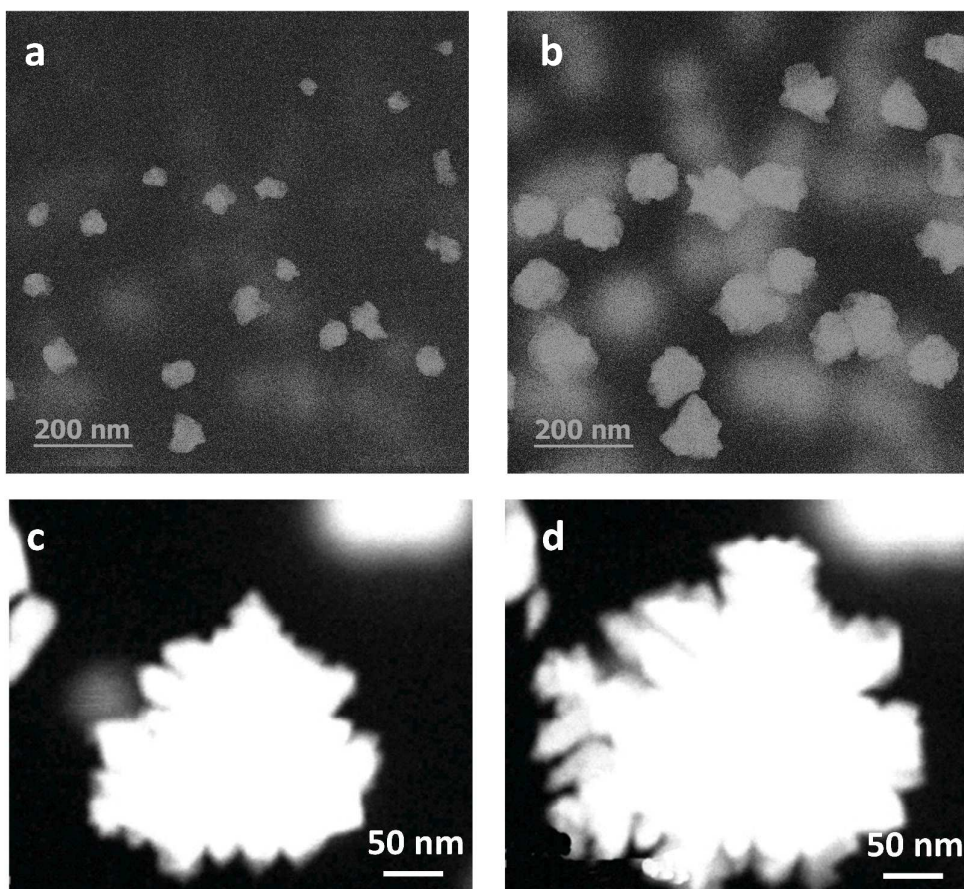
Figure S4: Growth of Au NPs at higher magnification. Two snapshots of 3D NPs growth with 20 seconds time interval acquired at (a-b) 250 k and (c-d) 400 k magnifications. We systematically observed the formation of branched 3D NPs at 250 k, while dendritic growth occurs at 400k.
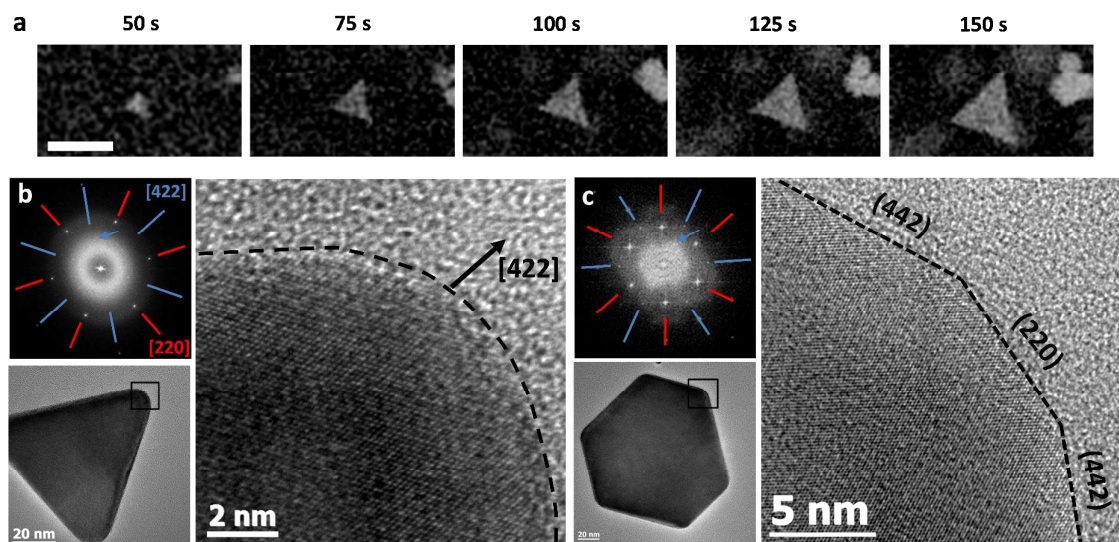
Figure S5: (a) *In situ* follow-up of the growth of a nanoprism keeping its triangular morphology all over the experiment. The irradiation time on the analysed area is indicated above each image and the scale bar corresponds to 100 nm (100k magnification). Detailed HRTEM analyses of faceting in (b) a nanoprism and (c) a planar nano-hexagon. Bottom and top left images are the images and corresponding FFTs of the nanoplates. The [220] and [422] crystallographic directions are indicated by red and blue lines, respectively. The blue arrow indicates the theoretically forbidden 1/3 422 reflection. Right images are magnified HRTEM micrographs of the nanoplate's corner indicated on left image. As illustrated here, nanoprisms exhibit rounded corners with no faceting perpendicular to the [422] directions, whereas the corners of planar hexagons present small (220) facets (or edges).

Video file:

A video file of NPs growth accelerated 4 times and acquired with a magnification of 100k (dose rate of 10^6 Gy/s) is available free of charge via the Internet at http://pubs.acs.org